Hindawi
Scientific Programming
Volume 2021, Article ID 9301571, 7 pages
https://doi.org/10.1155/2021/9301571

Research Article

Detection, Integration, and Optimization of Acoustic Field Simulation in the Closed Space

Siming Meng,[1] **Ge Lin**,[2] **and Xiaoyan Liang**[2]

[1]*Information Engineering Institute, Guangzhou Railway Polytechnic, Guangzhou 510430, China*
[2]*Sun Yet-sen University, Guangzhou 510006, China*

Correspondence should be addressed to Siming Meng; mengsiming@gtxy.edu.cn

Received 3 June 2021; Revised 23 June 2021; Accepted 29 July 2021; Published 24 August 2021

Academic Editor: Bai Yuan Ding

Noise pollution in the closed space such as railway carriage is an important problem because the noise pollution seriously affects comfort and health of people in the closed space. We propose the method to detection, integration, and optimization of acoustic field simulation in the closed space. First, we analyze the acoustic field distribution in the virtual 3D close space. We use harmonic sound wave propagation in the closed space and present the distribution according to geometric analysis. Second, we introduce Delaunay triangulation and k-means clustering into visualization to form the quiet zone and show it in 3D perspective. Our method used acoustic simulation to develop the sound barrier system. The simulation results show that our method can improve the analysis of the noise problem in the closed space.

1. Introduction

The problem of noise in the closed space such as railway carriage is an important problem. It not only seriously affects the passengers' comfort but also damages their health. The researches study various methods to deal with the problem of noise pollution in the close space. The virtual sound barrier system (VSB-S) method [1–3] is the interesting method to improve the acoustic environment. VSB-S uses the acoustic interference method to eliminate noise pollution in the close space, so it will not disturb the space at all. In VSB-S, the noise sensor array [4] is used to obtain spatial noise distribution, and the sound waves of the same amplitude and opposite phase to the noise are emitted to counteract the noise. We call the area in the space of sound counteract is the quiet zone.

In general, wave-based methods and geometric methods [5] are used for sound propagation in the close space. The wave-based methods built solve the acoustic wave equations [6–8]. However, it is very slow to solve the problem of the high frequency sound source or open sound field. This is because the computational complexity of this method is proportional to the volume of the sound field space and the fourth power of the maximum sound frequency. The geometric method uses straight line ray to describe sound propagation approximately [9]. We assume that noise is always along the ray propagation; the tangent direction of every point on ray is the direction of transmission of sound waves. The geometric acoustic methods usually cannot be described and are solved accurately by explicit equations, but they can efficiently simulate the sound transmission if ignored the reflected sound waves. So, we introduce the geometric acoustic approach for analysis of the acoustic field in a closed space.

On the basis of acoustic simulation, we use the computer simulation model to establish visual description of the sound field [10, 11]. Our method considers direct sound, reflected sound, and sound attenuation. We use the Delaunay triangulation model to get the silent area of VSB-S and use three-dimensional perspective to display the triangulation results. This study' contributions include two parts. First, we research the problem of sound comfort. In the past, the research on acoustics of the enclosed space mainly focused on hall acoustics and architectural acoustics. Then, the Delaunay triangulation method is preferred into wave-based acoustics to form the quiet zones in the enclosed space such

as railway carriage. We obtain a better subdivision result because of the application of the k-means clustering algorithm.

2. Related Work

Various methods have been proposed for the construction of the VSB system and visualization of sound field distribution. Due to the complexity of different types of sound waves and the multilateral nature of sound field environment, there is no simulation model that can adapt to all situations [12].

2.1. VSB System (VSB-S). Qiu et al. [1] used a group of loudspeaker arrays to build a virtual acoustic barrier applied to the driver's seat. They solve the problem of conflict with human's head using virtual sensor technology. Seyedin and Abedi [13] calculate sound propagation with complete reflection of sound waves from the walls by the FDTD method and estimate optimal amplitude to build the VSB system.

2.2. Sound Field Distribution Simulation. The technology of sound field [14–17] prediction in the closed space based on geometric acoustics is relatively mature and has been applied in many scenes. In a study [9], Cai et al. proposed a ray tracing method based on space partition to simulate the sound field in a closed space. In his method, the whole closed space is divided into finite convex polyhedral subspaces, so as to reduce the times of ray and wall intersection. In order to simplify the calculation, his method omits the validation of the collision point between the ray and the wall.

Based on the numerical method of sound wave propagation, equation is discretized, and then, the numerical calculation is carried out to approximate the solution [6]. There are many feasible methods to solve the wave equation, which are suitable for different application scenarios. The method of time domain solution (TDS) [7] depends on spatially invariant speed of sound. The method of an equivalent staggered grid scheme (ESG) [8] relies on variable density media. The adaptive rectangular decomposition method (ARD) [18] can combine the analytical solution of the rectangular subdomain wave equation with the finite difference template of interface processing between subdomains, so as to achieve high performance simulation with low error. A method of sound field simulation for spatial convolution circular array based on discrete Fourier transform (DFT) is proposed by Haneda et al. [19]. Tkamisinski [20] mentioned a visual simulation technology to analyze the influence of sound wave diffusion on music.

2.3. Delaunay Triangulation. Delaunay triangulation is a commonly used optimal triangulation method, which is widely used in mesh generation and surface reconstruction of a 3D scattered point set. It is one of the important research contents in CAGD, CGM, and CG. Delaunay triangulation has many advantages, such as maximizing the minimum angle and ensuring convergence. So, it can build the low complexity and high-quality mesh in the 3D space. Delaunay triangulation is the most popular surface generation method and has a widespread application. Wang and Wu [21] and Turnbull et al. [22] used Delaunay triangulation to describe the water surface, for visible analyzing the interactions of water waves or others obstacle interfere. Yu et al. [23] showed a 3D geological modeling of Nanjing City used the Delaunay triangulation method.

2.4. Clustering Algorithm. Cluster analysis is an important method of data division or grouping. Common clustering methods include k-means, density-based clustering, maximum expectation clustering, hierarchical agglomerative clustering, and graph detection clustering. These cluster algorithms are proposed to solve different practical problems. Likas et al. [24] proposed a global clustering method. Through the deterministic global search process composed of dataset size, a cluster center is dynamically added in one search process to achieve global optimization. Accordingly, we use the k-means cluster algorithm [25] based on Euclidean distance in this study, with the number of clusters to ensure the precise zones.

We demonstrate the sound field distribution in close space slice as shown in Figure 1. The first line is with two sound sources while the second line is with three. In Figure 1, we use yellow point sign point noise source.

3. The Modeling of the Sound Field

In this study, we use a virtual closed cuboid space to simulate the sound field space [26]. In order to simplify the simulation modeling, we assume that there are no other obstacles and other interference sound sources in the space.

Our study uses a 7 m × 5 m × 3 m cuboid to describe our virtual sound field space. Assuming that all the boundaries in the closed space are smooth rigid bodies, there is no diffuse reflection because it is so complex in our model [27]. At the same time, no other object in this virtual space should absorb or reflect the sound waves. Without considering any absorption and reflection, the sound propagation path between two points in the close space is a straight line.

The sound wave of the spherical point source propagates in the virtual space, and each point on the sound wave propagates on the uniform spherical surface in a certain period of time until it collides with the boundary of the space and reflects. Considering the complexity of the simulation model, when the noise reaches the boundary and reflects, we only consider the influence of the first radiated sound wave and ignore other sound waves.

3.1. Wave Equation of Sound. In this study, the sound field generated by a stable point source propagating in a closed space is studied. Through Fourier analysis [28], we can use some simple harmonic functions with different frequencies to express the acoustic vibration function. Therefore, the variation of the harmonic field with time is the basis of analyzing the variation of complex field with time. At any points in this closed space, the vibration information of the selected sound source [29, 30] is as follows:

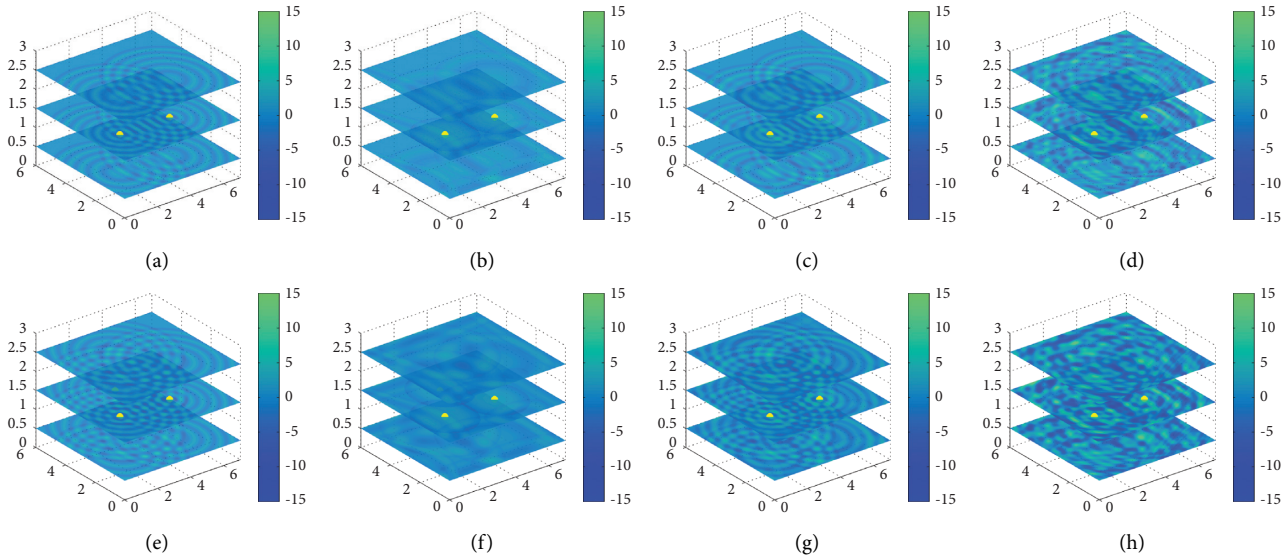

Figure 1: Examples of sound field distribution. The first line is with two sound sources while the second line is with three. Yellow points are sound source locations.

$$P(x, y, z; t) = e^{-2\alpha\gamma} A_0 \cos[w(t - t_0) + \varnothing_0], \quad (1)$$

where $t_0 = r/v$ is the time of sound wave transmission in the close space, r is the distance, v is the speed of sound in air, $t - t_0$ means that the vibration of the sound wave is beginning from the moment it spread to here, $\varnothing_0$ is the initial phase of the sound wave, and α is an attenuation factor.

3.2. Sound Wave Reflection. It will get many reflected sound waves when reaching boundary in space. Figure 2 shows intersection of spherical sound waves from multiple point sources. Figure 2(a) shows spherical sound waves intersection from 2 point sources, and Figure 2(b) shows spherical sound waves intersection from 3 point sources. There are many factors affecting the sound field distribution. The sound field distribution after impact reflection is affected not only by the propagation direction of the point source but also by the propagation attenuation.

In our model, all the boundaries are smooth rigid bodies. After the point source sound waves collide and reflect on the boundary surface, they will be reflected at the same angle as the incident angle. Therefore, at any point in the close space, the value of acoustic intensity will be equal to the direct sound at that point and all the values reflected by all boundaries. In this study, the closed space environment is simulated as a virtual cuboid, and the boundary is regarded as a rigid reflector. In this way, we can ignore all kinds of attenuation [31–33] and only consider the boundary reflection.

3.3. Sound Wave Interference in the Closed Space. A single proton vibrates longitudinally in a spherical acoustic wave. When sound waves with the same vibration frequency and amplitude collide, a superimposed energy will be produced. If the two protons vibrate in the opposite direction, the energy will cancel each other. We use p_1 and p_2 that express sound pressures of two sound waves, and the synthetic sound field pressure is p. It can be calculated by the following formulas:

$$\nabla^2 (p_1 + p_2) = \frac{1}{c_0^2} p_1 \frac{\partial^2 (p_1 + p_2)}{\partial t^2}, \quad (2)$$

$$\nabla^2 (p_i) = \frac{1}{c_0^2} \frac{\partial^2 (p_i)}{\partial t^2}. \quad (3)$$

4. Quiet Area Integration

We detect the collision point by the feature of sparse and dense in the propagation of the point source. Then, we introduce Delaunay triangulation to represent the final quiet region due to the regularity and uniqueness of the surface formed by collision points. Finally, we use Euclidean distance for k-means clustering [34] to improve the final results.

4.1. Detection of Impact Points. We assume that there are three sound source points in the closed space, and the frequency and amplitude of the sound source are the same. According to the stability of direct sound and the change of reflected sound, the collision position of sound wave in the space can be calculated [35, 36]. We consider the area of 1.0-2.0 meters in the vertical direction is our "sweet area." We discretize the sound field space and get the acoustic impact point through the sparse and dense characteristics of the discrete points.

4.2. Quiet Area Integration. It is difficult to triangulate discrete points in space. The constancy of coherent wave provides a strong guarantee for our work. By controlling the wave length, we can get a good triangulation dataset.

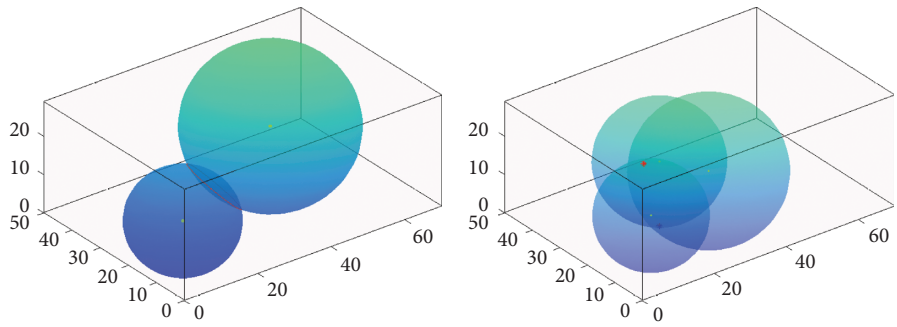

Figure 2: Intersection of spherical sound waves from multiple point sources. (a) Spherical sound waves intersection from 2 point sources, yellow points represent the locations of sound sources. (b) Spherical sound waves intersection from 3 point sources.

First, a super triangle is created to contain all the scattered points in the triangle list. Second, insert points one by one, find the triangle whose circumscribed circle contains the insertion point from the triangle list, and delete the common edge that has influence on it. Connect the insertion point with all the vertices of its related triangle to complete the insertion point into the Delaunay triangle list. Then, the new local triangles are optimized according to the optimization rules, and the generated triangles are put into the Delaunay triangle table. Loop the insertion until all points are inserted. Two triangular subdivision surfaces in the 3D space can be on the same plane. Let us first draw in two dimensions. During this process, some points may be deleted because they are on a line that is not referenced by triangulation.

The Delaunay triangulation result is shown in Figure 2.

4.3. Subzone Dividing. The impact point set we get from section discrete point detection may be distributing across the space sparsely [37, 38] or forming several dense parts distinctly. If we generate the quiet zones on the impact point set directly, we may get a surface that almost covers the whole space, which make our study become meaningless. In order to avoid this situation, we introduce the clustering algorithm before Delaunay triangulation to create space subsets. We implement surface subdivision from the subsets. With this method, we may get several precise quiet zones. We employ Euclidean distance to be the unique attribute work on the clustering algorithm. Any clustering algorithm can be used to obtain the final grouping of elements. We use the k-means algorithm to achieve data partition.

Iterating according to the following formulas could get labeling the initial dataset u.

$$C^{(i)} = \operatorname{argmin}_j \left| d^{(i)} - u_j \right|^2, \tag{4}$$

where $d^{(i)}$ and u_j are the spatial coordinates vector. Its main point is to apply the distance between the original dataset and the initialization random data. Then, find out the data with the nearest distance to the initial data:

$$u_j = \frac{\sum_{i-1}^{m} l\{c^i = j\} d^i}{\sum_{i-1}^{m} l\{c^i = j\}}. \tag{5}$$

This formula aims at getting the average distance between all the original data and one initial data. Iterate the two formulas until the member in set u do not change anymore, and we get the labeling group dataset.

5. Experimental Results

5.1. Sound Field Distribution. Our approach obtains the visualization through the discrete points detection. When we calculate sound pressure of one point, we only consider the direct sound and the primary reflection. All boundaries we simulate are idealized rigid edge, and we do not put the fact into consideration that sound wave reflect from a wall would product a series of wavelet, which may cause standing wave in the whole space and diminish the reflection value [39–43]. Therefore, each time we calculate sound pressure of one point, and we should put the three direct sound and eighteen reflections into consideration. The two and three spherical waves intersection is shown in Figure 2.

We collect a data point per cubic decimeter; then, we have 118059 data to deal with. Figure 3 shows the results of visualization simulation and Delaunay triangulation [44, 45]. The first line shows the situation about two sound sources while the second line is about three. The first three columns are 0.001 s when the sound is not spreading in the whole room yet. The last column is 0.005 s when the room is full of sound waves. The third column is the sum of the first two columns. We could see that the first column is almost exactly the same with the third column because the value of reflection is so small to affect the entire waveform. But we could see that the waveform was not irregular anymore when time is at 0.005 s because of the strong reflection.

In our experiment, sound field distribution of a whole space in Figures 3(a) and 3(d) will cost about 1 and a half minutes, computing on the 64 bits system of Intel CPU, 16G RAM per time. Illustrated in Figures 3(a) and 3(d), through simulation, the distribution of sound field in space is visualized. Different sound intensities are marked with different colors.

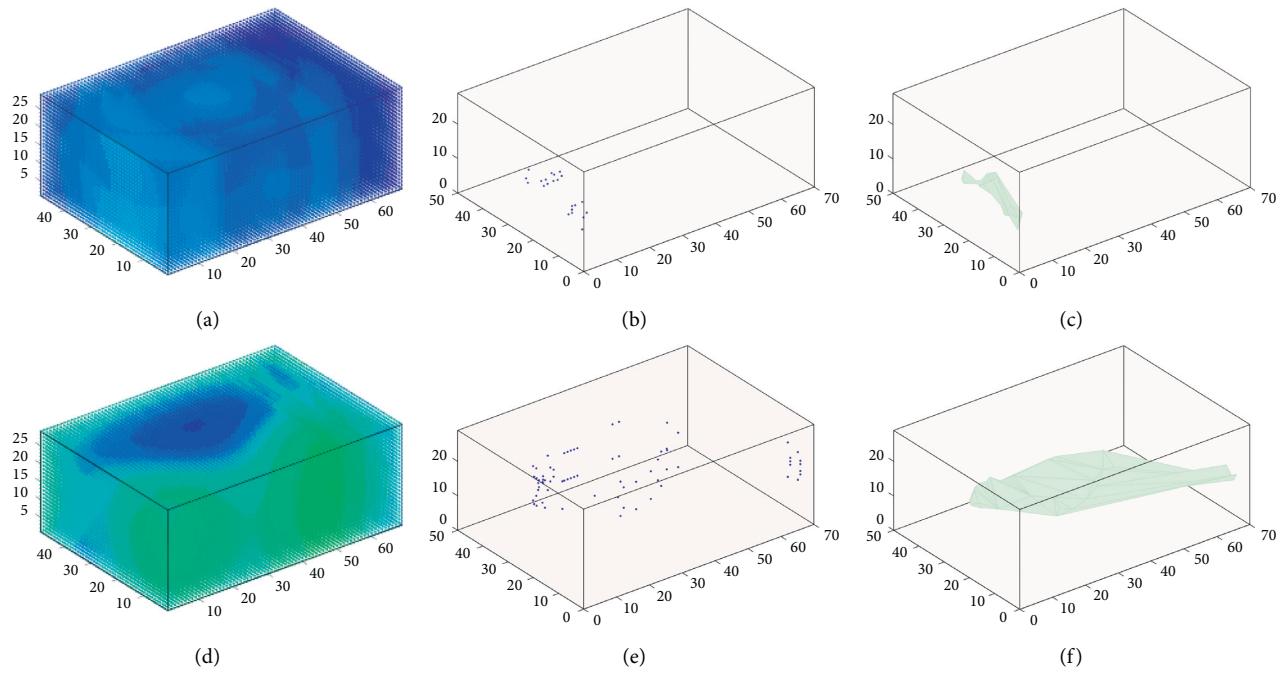

Figure 3: The results of visualization simulation and Delaunay triangulation. (a), (d) The distribution in $t = 0.01$ s and $t = 0.05$ s. (b), (e) The dataset of impact points in $t = 0.01$ s and $t = 0.05$ s. (c), (f) The Delaunay triangle surface in $t = 0.01$ s and $t = 0.05$ s.

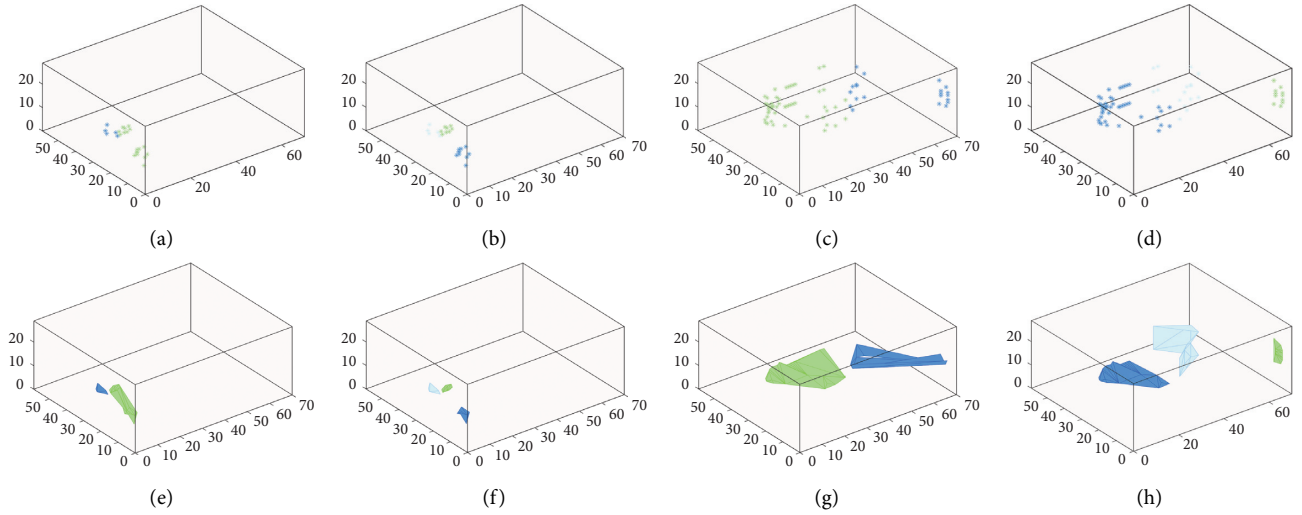

Figure 4: The results of cluster. (a)–(d) Cluster results of impact points at 0.01 s and 0.05 s. (e)–(h) Their cluster respective subdivision results.

5.2. Impact Points Detection. We could simplify data detection. As shown in Figures 3(b) and 3(e), the amplitude of a point in vibration always approximate the point nearby because of the continuity of volatility. Because of this, there may be many impact points in a small region, which provides a powerful guarantee for Delaunay triangulation.

5.3. Delaunay Triangulation. We map the set into the 2D space primarily. As a result, not all the impact points would be the vertex of the Delaunay triangle. Figures 3(c) and 3(f) show the final result of subdivision, and it is obvious that some points have been removed. We can see the surface is so rough that it does not look like a zone.

5.4. Subzone Dividing. The k-means clustering algorithm is used to distinguish the collision point set. The initial class number K, namely, the desired number of clusters, must be confirmed before clustering, and it is the user to specify parameters [46]. When we call the k-means function to do with the impact point set, it need to iterate based on the initial value. Iteration will not stop until the cluster does not change anymore.

As shown in Figure 4, we could get different subdivision results with different K values. As for the situation about Figure 3(f), we could improve it in Figures 4(g) and 4(h). The quiet zone we get could not cover large areas of points with high sound pressure values, and get the quiet zones in a close space. Figures 4(a) and 4(b) are cluster results of impact points at 0.01 s, while Figures 4(e) and 4(f) are their respective subdivision results. The others are time at 0.05 s.

6. Conclusion

With the problem of noise in closed a three-dimensional space, a simulation model of spherical wave propagation and interaction formed by multiple point sound sources is proposed and used to calculate the quiet area of the closed space. First, we analyze the sound field in a closed space with the geometric acoustics method and describe the intensity of the sound field with a color map. Second, Delaunay triangulation is introduced into the simulation, and finally, the quiet area is optimized by clustering.

First, we use the geometric wave acoustic analysis method to calculate the propagation of spherical sound wave, mainly considering the boundary reflection of smooth rigid body, analyzing the sound field distribution of a multipoint sound source and using the discrete method to detect the collision point. Then, Delaunay triangulation is used to form a continuous surface in the quiet area. Finally, the k-means clustering algorithm is used to optimize the quiet area. In the experiment, we give the visual description of different time and sound sources. The simulation results show that geometric analysis can directly and effectively analyze sound field distribution.

In the future research, we will learn from the near space physical signal acoustic suppression processing system and modify the experimental parameters according to the actual measurement data, so that the system has a practical application value. At the same time, we will verify the effectiveness of the model in complex noise scenes such as train compartments.

Data Availability

The dataset used to support the findings of this study is publicly available.

Conflicts of Interest

The authors declare that they have no conflicts of interest.

Acknowledgments

The research was supported by Newly Introduced Talents Scientific Research Start-Up Project of Guangzhou Railway Polytechnic (GTXYR1801).

References

[1] X. Qiu, N. Li, and G. Chen, "Feasibility study of developing practical virtual sound barrier system," in *Proceedings of the 12th International Congress on Sound and Vibration*, Lisbon, Portugal, July 2005.

[2] H. Zou, X. Qiu, J. Lu et al., "A preliminary experimental study on virtual sound barrier system," *Journal of Sound and Vibration*, vol. 307, no. 1, pp. 379–385, 2007.

[3] H. Zou and X. Qiu, "Performance analysis of the virtual sound barrier system with a diffracting sphere," *Applied Acoustics*, vol. 69, no. 10, pp. 875–883, 2008.

[4] H. Zou, X. Qiu, F. Niu, and J. Lu, "A numerical and experimental study on virtual sound barrier," *Acta Acoustica*, vol. 32, no. 1, pp. 26–33, 2007.

[5] L. Antani, A. Chandak, and M. Taylor, "Direct-to-Indirect acoustic radiance transfer," *Visualization and Computer Graphics*, vol. 18, no. 2, pp. 261–269, 2011.

[6] N. Raghuvanshi, N. Galoppo, and M. C. Lin, "Accelerated wave-based acoustics simulation," in *Proceedings of the 2008 ACM symposium on Solid and physical modeling*, pp. 91–102, ACM, Stony Brook, NY, USA, June 2008.

[7] R. Mehra, N. Raghuvanshi, L. Savioja, M. C. Lin, and D. Manocha, "An efficient GPU-based time domain solver for the acoustic wave equation," *Applied Acoustics*, vol. 73, no. 2, pp. 83–94, 2012.

[8] L. Di Bartolo, C. Dors, and W. J. Mansur, "A new family of finite-difference schemes to solve the het-erogeneous acoustic wave equation," *Geophysics*, vol. 77, no. 5, pp. 187–199, 2012.

[9] M. Cai, Z. Chen, and J. Zou, "A ray tracing method based on indoor space partition-ing," *Applied Acoustics*, vol. 32, no. 1, pp. 34–38, 2013.

[10] X. Wang, X. Liu, Q. Zou, and L. Ge, "Multichannel LMS-based large area sound inhibition in home environment: preliminary simulation and experiments," in *Proceedings of the International Conference on Digital Home*, pp. 401–405, Guangzhou, China, November 2014.

[11] X. Liu, Q. Zou, X. Wang, and L. Ge, "Acoustic feedback effect reduction based on path compensation in multichannel FXLMS sound in-hibition systems," in *Proceedings of the International Conference on Digital Home*, pp. 390–394, Guangzhou, China, November 2014.

[12] Q. Q. Li, C. Ripamonti, and R. Caccialanza, "Simulation of deterministic tyre noise based on a monopole substitution model," *Applied Acoustics*, vol. 178, 2021.

[13] S. A. Seyedin and M. H. Abedi, *Optimizing Secondary Source Location in Acoustic ANC Systems*, IEEE, Manhattan, NY, USA, 2006.

[14] T. Jasa and N. Xiang, "Nested sampling applied in Bayesian room-acoustics decay analysis," *Journal of the Acoustical Society of America*, vol. 132, no. 5, pp. 3251–3262, 2012.

[15] K. Kowalczyk and M. Van Walstijn, "Room acoustics simulation using 3-D compact explicit FDTD schemes," *IEEE Transactions on Audio Speech and Language Processing*, vol. 19, no. 1, pp. 34–46, 2011.

[16] C. J. Webb and S. Bilbao, "Computing room acoustics with CUDA-3D FDTD schemes with boundary losses and viscosity," in *Proceedings of the Acoustics, Speech and Signal Processing (ICASSP), 2011 IEEE International Conference on*, pp. 317–320, Prague, Czech Republic, May 2011.

[17] D. T. Murphy, A. Southern, and L. Savioja, "Source excitation strategies for obtaining impulse responses in finite difference time domain room acoustics simulation," *Applied Acoustics*, vol. 82, pp. 6–14, 2014.

[18] L. Antani, A. Chandak, M. Wilkinson et al., "Validation of adaptive rectangular decomposition for three-dimensional wave-based acoustic simulation in architectural models,"

Proceedings of Meetings on Acoustics, vol. 19, no. 1, pp. 015–099, 2013.

[19] Y. Haneda, K. i. Furuya, S. Koyama, K. Niwa, and K. Kobayashi, "Sound field simulation for circular array based on spatial circular convolution," *Acoustical Science and Technology*, vol. 35, no. 2, pp. 99–107, 2014.

[20] T. Kamisinski, "Acoustic simulation and experimental studies of theatres and concert Hall-s," *Acoustic and Biomedical Engineering*, vol. 118, no. 1, pp. 78–82, 2010.

[21] C. Z. Wang and G. X. Wu, "Interactions between fully nonlinear water waves and cylinder arrays in a wave tank," *Ocean Engineering*, vol. 37, no. 4, pp. 400–417, 2010.

[22] M. S. Turnbull, A. G. L. Borthwick, and R. Eatock Taylor, "Wave-structure interaction using coupled structured-unstructured finite element meshes," *Applied Ocean Research*, vol. 25, no. 2, pp. 63–77, 2003.

[23] S.-J. Yu, F. Guo, L. Xiang, and F. Xu, "Application of constrained Delaunay tetrahedralization in 3D geological modeling," *Geography and Geo-Information Science*, vol. 29, no. 1, pp. 41–44, 2013.

[24] A. Likas, N. Vlassis, and J. Verbeek, "The global k-means clustering algorithm," *Pattern Recognition*, vol. 36, no. 2, pp. 451–461, 2003.

[25] G. H. Du, Z. M. Zhu, and X. Gong, *Fundamentals of acoustics*, Press of Nanjing University, Nanjing, China, 2012.

[26] E. Deines, M. Bertram, J. Mohring et al., "Comparative visualization for wave based and geometric acoustics," *Visualization and Computer Graphics*, vol. 14, no. 6, pp. 1707–1722, 2008.

[27] S. Siltanen, T. Lokki, S. Tervo, and L. Savioja, "Modeling incoherent reflections from rough room surfaces with image sources," *Journal of the Acoustical Society of America*, vol. 131, no. 6, pp. 4606–4614, 2012.

[28] A. Torras-Rosell, S. Barrera-Figueroa, and F. Jacobsen, "Sound field reconstruction using acousto-optic tomography," *Journal of the Acoustical Society of America*, vol. 131, no. 5, pp. 3786–3793, 2012.

[29] J. Yu, H. Pu, J. Chen, and S. Lu, "The measurement of sound speed and the study of sound waves," *College Physics*, vol. 26, no. 1, pp. 58–61, 2007.

[30] Y. Ji, H. Pu, J. Chen, and S. Lu, "The measurement of sound speed and the study of sound waves," *College Physics*, vol. 26, no. 1, pp. 58–61, 2007.

[31] W. Rao, "A study of effects of boundary and directional sound sources on virtual sound v-barrier system," Master's thesis, Master's thesis of Nanjing university, Nanjing, China, 2011.

[32] J. Peng, "Finite difference time domain method and its application in room acoustical simulation," *Technical Acoustics*, vol. 28, no. 1, pp. 53–57, 2009.

[33] G. Yan and J. Lin, "Continuous element for 1D problems," *Partial Differential Equations and the Finite Element Method*, vol. 21, no. 1, pp. 45–102, 2005.

[34] A. Likas, N. Vlassis, and J. Verbeek, "The global k-means clustering algorithm," *Pattern Recognition*, vol. 36, no. 2, pp. 451–461, 2003.

[35] S. Yu, F. Guo, X. Li, and F. Xu, "Application of constrained Delaunay tetrahedralization in 3D geological modeling," *Geography and Geo-Information Science*, vol. 29, no. 1, pp. 41–44, 2013.

[36] A. Bassuet, D. Rife, and L. Dellatorre, "Computational and optimization design in geometric acoustics," *Building Acoustics*, vol. 21, no. 1, pp. 75–86, 2014.

[37] W. Han, X. Bu, and M. Xu, "Yunpu Zhu Model of a surface acoustic wave sensing system based on received signal strength indication detection," *Measurement Science and Technology*, vol. 32, no. 8, pp. 85–103, 2021.

[38] E. Vevek and W. L. Chan, "Adomain decomposition technique for small amplitude wave interactions with shock waves," *Journal of Computational Physics*, vol. 437, 2021.

[39] C. Chen, T. Chen, and Y. Wang, "Observation of topological locally resonate and Bragg edge modes in a two-dimensional slit-typed sonic crystal," *Applied Physics Express*, vol. 12, no. 9, Article ID 097001, 2019.

[40] J. Lu, C. Qiu, L. Ye et al., "Observation of topological valley transport of sound in sonic crystals," *Nature Physics*, vol. 13, no. 4, pp. 369–374, 2017.

[41] S. Kang and J. Hwang, "Tuning the characteristics of photoacoustic pressure in a laser-induced photoacoustic generator: a numerical study," *Applied Mathematical Modelling*, vol. 94, pp. 98–116, 2021.

[42] J. Liu, J. Du, J. Wang, and J. Yang, "Effects of surface impedance on current density in a piezoelectric resonator for impedance distribution sensing," *Applied Mathematics and Mechanics*, vol. 42, no. 5, pp. 677–688, 2021.

[43] J. Liu, J. Du, J. Wang, and J. Yang, "Thin film bulk acoustic wave piezoelectric resonators with circular ring driving electrodes for mass sensing," *Integrated Ferroelectrics*, vol. 192, no. 1, pp. 57–66, 2018.

[44] P. Caday, M. V. de Hoop, V. Katsnelson, and G. Uhlmann, "Recovery of discontinuous Lame parameters from exterior Cauchy data," *Communications in Partial Differential Equations*, vol. 46, no. 4, pp. 680–715, 2020.

[45] S. Kugunavar and C. J. Prabhakar, "Content-based medical image retrieval using Delaunay triangulation segmentation technique," *Journal of Information Technology Research*, vol. 14, no. 2, pp. 48–66, 2021.

[46] K. Trojachanec, I. Kitanovski, I. Dimitrovski, and S. Loshkovska, "Longitudinal brain MRI retrieval for alzheimer's disease using different temporal information," *IEEE Access*, vol. 6, pp. 9703–9712, 2018.